SIAM J. Applied Dynamical Systems
Vol. 8, No. 2, pp. 689–709

Discrete Traveling Solitons in the Salerno Model*

Thomas R. O. Melvin†, Alan R. Champneys†, and Dmitry E. Pelinovsky‡

Abstract. We investigate traveling solitary waves in the one-dimensional (1D) Salerno model, which interpolates between the cubic discrete nonlinear Schrödinger (DNLS) equation and the integrable Ablowitz–Ladik (AL) model. In a traveling frame the model becomes an advance-delay differential equation to which we analyze the existence of homoclinic orbits to the rest state. The method of beyond all orders asymptotics is used to compute the so-called Stokes constant that measures the splitting of the stable and unstable manifolds. Through computing zeros of the Stokes constant, we identify a number of solution families that may bifurcate for parameter values between the DNLS and AL limits of the Salerno model. Using a pseudospectral method, we numerically continue these solution families and show that their parameters approach the curves of the zero level of the Stokes constant as the soliton amplitude approaches zero. An interesting topological structure of solutions occurs in parameter space. As the AL limit is approached, solution sheets of single-hump solutions undergo folds and become double-hump solitons. Numerical simulation suggests that the single-humps are stable and interact almost inelastically.

Key words. discrete nonlinear Schrödinger equation, Salerno model, traveling wave solutions, beyond all orders asymptotics, computations of Stokes constants

AMS subject classifications. 34K28, 35Q55, 37K60, 34M40

DOI. 10.1137/080715408

1. Introduction.

The existence of localized traveling waves in discrete nonlinear Schrödinger (DNLS) lattices has recently received a lot of attention (see, e.g., [8]). This is largely due to the experimental realization of solitons in discrete media, such as waveguide arrays [3] and optically induced photorefractive crystals [9]. The prototypical equation that emerges from these models is the DNLS equation with some nonlinear term f, of the form

$$i\dot{u}_n(t) = \frac{u_{n+1}(t) - 2u_n(t) + u_{n-1}(t)}{h^2} + f(u_{n+1}(t), u_n(t), u_{n-1}(t)). \tag{1.1}$$

Finding traveling solitons which move without shedding any radiation, that is, homoclinic orbits to the rest state in a moving frame, is a very delicate problem. Analyzing traveling solutions with small wavespeed that bifurcate from the stationary solutions is problematic, as moving into the traveling frame introduces a large number of resonances in the spectrum of the linear operator which give rise to radiation modes. To minimize the number of these radiation modes it is necessary to look for solutions that travel with a *finite* wavespeed [13],

*Received by the editors February 11, 2008; accepted for publication (in revised form) by T. Kaper February 23, 2009; published electronically June 3, 2009. This work was supported by the UK EPSRC.
http://www.siam.org/journals/siads/8-2/71540.html
†Department of Engineering Mathematics, University of Bristol, Bristol BS8 1TR, United Kingdom (thomas.melvin@metoffice.gov.uk, a.r.champneys@bristol.ac.uk).
‡Department of Mathematics, McMaster University, Hamilton, Ontario, Canada, L8S 4K1 (dmpeli@math.mcmaster.ca).

that is, in an appropriate region of parameter space where the minimum wavespeed is bounded away from zero. However, posing the DNLS in a traveling frame gives rise to a differential advance-delay equation which is notoriously hard to analyze. Recent progress in this area has been made by developing a Melnikov method around existing solution families [18] or by using a pseudospectral method to transform the advance-delay equation into a large system of algebraic equations [2, 14]. Alternatively, looking for small-amplitude (but nonzero wavespeed) solutions bifurcating from the rest state involves computation of the so-called Stokes constants [22] in the method of beyond all orders asymptotics, which measures the splitting of the stable and unstable manifolds. This problem was considered in [15] for the DNLS with a saturable nonlinear term, where a number of zeros of the Stokes constant were found for a sufficiently large saturation parameter. This paper concerns derivation and computation of the Stokes constant for the Salerno model [21] with the nonlinear function

$$f = 2(1-\alpha)\,|u_n|^2\,u_n + \alpha\,|u_n|^2\,(u_{n+1}+u_{n-1}). \tag{1.2}$$

The Salerno model is a DNLS equation which interpolates between the cubic DNLS model [12] at $\alpha = 0$ and the integrable Ablowitz–Ladik (AL) model [1] at $\alpha = 1$. The Salerno model was also derived from the Gross–Pitaevskii equation for Bose–Einstein condensates with magnetic momentum [11]. It is well known [19] that no single-humped localized traveling waves exist in the DNLS with pure cubic nonlinearity, $\alpha = 0$, because single-humped solitons are surrounded by nondecaying oscillatory tails. However, models with other discretizations of the cubic term in the DNLS equation often support localized traveling waves. These include the AL lattice [10] and the lattice with translationally invariant stationary solutions derived in [17]. The Salerno model has a two-parameter family of exact traveling solitary wave solutions at $\alpha = 1$ corresponding to the AL lattice; however, these solutions do not persist for $\alpha \neq 1$ away from the integrable limit [10]; this result has been confirmed using a Melnikov method in [18]. However, further numerical results in [18] suggest that the Salerno model can still support traveling solutions for some $\alpha \neq 1$ far from the integrable limit. The existence of traveling waves in the Salerno model for $\alpha \in (0, 1)$ is the subject of this paper.

The paper is organized as follows. In section 2 we derive a regular asymptotic solution to the Salerno model in the continuous limit, when the advance-delay operator is formally replaced by the series of differential operators. Although this solution is correct to all orders of the asymptotic expansion, it does not capture the radiation tails, as these terms are exponentially small in the bifurcation parameter and hence lie beyond all orders of the expansion. In section 3 we use the method of beyond all orders asymptotics (see [15, 22] and references therein) to analytically continue the expansion into the complex plane, where the asymptotic expansion blows up. The Stokes constants measure the residue coefficients of the singular part of the beyond all orders terms corresponding to the splitting between stable and unstable manifolds. Section 4 deals with computation of the Stokes constant in the region of parameter space where there is only one radiation mode. We find that for suitable parameter values there exist a number of zeros of the Stokes constant which may indicate bifurcations of traveling wave solutions to the Salerno model. Using a pseudospectral method [6, 7] in section 5, we compute the traveling solitons and show that their parameters approach the curves for the zero level of the Stokes constant as the soliton amplitude approaches zero. Finally, we sum up our conclusions and discuss open problems in section 6.

2. Regular asymptotic expansion. Taking (1.1), we look for traveling solutions of the form

$$u_n(t) = \phi(hn + 2ct)e^{-i\omega t}, \qquad \phi : \mathbb{R} \mapsto \mathbb{C}, \quad \omega, c \in \mathbb{R},$$

where ω is the temporal frequency and c is the wavespeed of the traveling solutions. Moving into the traveling frame $z = hn + 2ct \in \mathbb{R}$ gives the differential advance-delay equation,

$$2ic\phi'(z) = \frac{\phi(z+h) - 2\phi(z) + \phi(z-h)}{h^2} - \omega\phi(z) + f(\phi(z+h), \phi(z), \phi(z-h)), \tag{2.1}$$

where f is given by (1.2) for the Salerno model. We are interested in localized solutions to (2.1), i.e., modes for which $\phi(z) \to 0$ as $z \to \pm\infty$. It is convenient to use the transformation of variables,

$$\phi(z) = \frac{\kappa}{h}\Phi(Z)e^{i\beta Z/\kappa}, \quad z = \frac{hZ}{\kappa}, \tag{2.2}$$

and the parameterization

$$\omega = \frac{2}{h}\beta c + \frac{2}{h^2}\left[\cos(\beta)\cosh(\kappa) - 1\right], \quad c = \frac{1}{h\kappa}\sin(\beta)\sinh(\kappa), \tag{2.3}$$

where $\kappa \in \mathbb{R}_+$ and $\beta \in [0, 2\pi]$. Substitution of (2.2)–(2.3) into (2.1) gives an equation for $\Phi(Z)$ in the form

$$\begin{aligned} &\cos(\beta)\left[\Phi(Z+\kappa) + \Phi(Z-\kappa) - 2\cosh(\kappa)\Phi(Z)\right] \\ &+ i\sin(\beta)\left[\Phi(Z+\kappa) - \Phi(Z-\kappa) - 2\sinh(\kappa)\Phi'(Z)\right] \\ &+ \kappa^2|\Phi(Z)|^2\left(2(1-\alpha)\Phi(Z) + \alpha(\Phi(Z+\kappa)e^{i\beta} + \Phi(Z-\kappa)e^{-i\beta})\right) = 0. \end{aligned} \tag{2.4}$$

Note that parameter h does not appear in the main equation (2.4) thanks to the scaling transformation (2.2)–(2.3).

Bifurcations of traveling wave solutions may occur in the limit $\kappa \to 0$ [19], where parameter κ corresponds to the smallest spatial decay rate of a traveling wave. The curve $\kappa = 0$ gives a boundary of the existence domain on the (ω, c)-plane shown in Figure 1, where the shaded region corresponds to imaginary values of κ. In the white region, the values of κ are real. On the boundary $\kappa = 0$, radiation modes are present for any $\beta \in [0, \pi]$ (if $c > 0$), and the number of radiation modes accumulate to infinity as $\beta \to 0$ or $\beta \to \pi$. There exist β_0 and β_1 such that $\beta_0 < \frac{\pi}{2} < \beta_1$, where the only radiation mode is present for $\beta \in (\beta_0, \beta_1)$. The points with $\kappa = 0$ and $\beta = \{\beta_0, \frac{\pi}{2}, \beta_1\}$ are shown on Figure 1 by arrows. At $\beta = \beta_0$ and $\beta = \beta_1$, additional bifurcation curves mark appearance of additional radiation modes, which exist inside the shaded region. We shall focus on the existence of traveling wave solutions in the white region outside the shaded area, since there exists only one radiation mode in the region.

The equation in the form (2.4) is said to be the outer equation for the bifurcation. We seek a regular asymptotic expansion of the outer equation in powers of κ. Compared to the standard continuous limit, where the expansions are performed in powers of lattice spacing h in the original equation (2.1), the small parameter κ serves the same purpose in the context

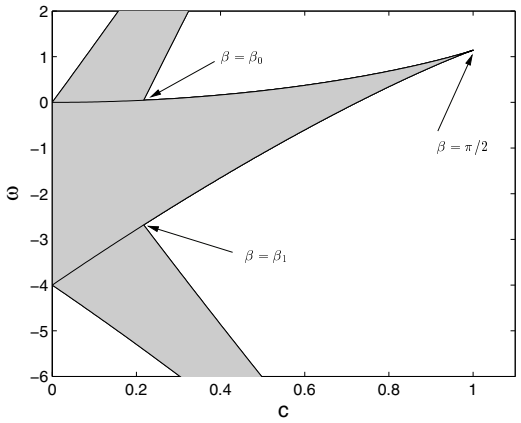

Figure 1. *Bifurcation curve $\kappa = 0$ on the (ω, c)-plane for $h = 1$. Localized solutions of the differential advance-delay equation (2.4) may bifurcate from the boundary to the white region. For $\beta < \beta_0$ and $\beta > \beta_1$, more than one radiation mode exists.*

of the normalized equation (2.4). The advance and delay terms are expanded in the power series,

(2.5)
$$\Phi(Z+\kappa) + \Phi(Z-\kappa) - 2\cosh(\kappa)\Phi(Z) = \kappa^2[\Phi''(Z) - \Phi(Z)] + \frac{\kappa^4}{12}[\Phi''''(Z) - \Phi(Z)] + O(\kappa^6),$$
$$\Phi(Z+\kappa) - \Phi(Z-\kappa) - 2\sinh(\kappa)\Phi'(Z) = \frac{\kappa^3}{3}[\Phi'''(Z) - \Phi'(Z)] + O(\kappa^5),$$

while the nonlinear function f is expanded as

(2.6)
$$f = 2[1 + \alpha(\cos(\beta) - 1)]\,|\Phi(Z)|^2\,\Phi(Z) + 2i\kappa\alpha\sin(\beta)\,|\Phi(Z)|^2\,\Phi'(Z) + \kappa^2\alpha\cos(\beta)\,|\Phi(Z)|^2\,\Phi''(Z) + O(\kappa^3).$$

We seek an outer asymptotic expansion for $\Phi(Z)$ of the form

(2.7)
$$\Phi(Z) = \sum_{n=0}^{\infty} (i\kappa)^n \Phi_n(Z).$$

Substituting this expansion into (2.4) gives, to leading order, $O(\kappa^2)$,

$$\cos(\beta)[\Phi_0''(Z) - \Phi_0(Z)] + 2[1 + \alpha(\cos(\beta) - 1)]\,|\Phi_0(Z)|^2\,\Phi_0(Z) = 0,$$

which has a real-valued solution

(2.8)
$$\Phi_0(Z) = S\,\mathrm{sech}(Z), \quad S = \frac{\sqrt{\cos(\beta)}}{\sqrt{1 + \alpha(\cos(\beta) - 1)}}$$

if $S \in \mathbb{R}$. The region of parameter space for which this holds, bounded by the curves $\beta = \frac{\pi}{2}$, $\beta = \beta^*(\alpha)$, and $\beta = \pi$, is shown in Figure 2, where $\beta^*(\alpha)$ is found from the equation

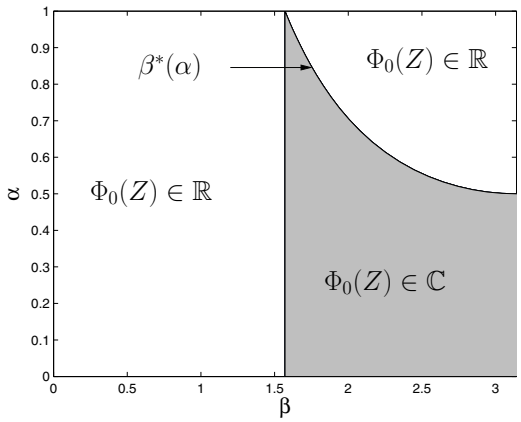

Figure 2. *Parameter regions, for which solution (2.8) is real-valued (white) and complex-valued (shaded).*

$1 + \alpha(\cos(\beta) - 1) = 0$.

At the next order, $O(\kappa^3)$, we obtain a linear inhomogeneous equation for a real-valued $\Phi_1(Z)$ in the form

$$\begin{aligned} L_- \Phi_1 &= \frac{\sin(\beta)}{3\cos(\beta)} \left(\Phi_0'''(Z) - \Phi_0'(Z) + 6\alpha |\Phi_0(Z)|^2 \Phi_0'(Z) \right) \\ &= \frac{2\sin(\beta) S^3 (1-\alpha)}{\cos^2(\beta)} \operatorname{sech}^3(Z) \tanh(Z), \end{aligned} \tag{2.9}$$

where $L_- = -\partial_Z^2 + 1 - 2\operatorname{sech}^2(Z)$. Since $L_- \Phi_0 = 0$ and $\Phi_0(Z)$ is an even function on $\mathbb{R}$, while the right-hand side of (2.9) is an odd function on $\mathbb{R}$, a unique odd solution exists for $\Phi_1(Z)$, in fact, in the explicit form

$$\Phi_1(Z) = \frac{\sin(\beta) S^3 (1-\alpha)}{2\cos^2(\beta)} \operatorname{sech}(Z) \tanh(Z).$$

Note that this term is zero for the AL lattice ($\alpha = 1$), as an exact solution of the differential advance-delay equation (2.4) with $\alpha = 1$ exists in the form $\Phi = \Phi_0(Z) = \operatorname{sech}(Z)$.

To compute the solution to higher orders, $O(\kappa^n)$ for $n \geq 4$, we have to solve a system of inhomogeneous linear equations separately in odd and even orders of n:

$$L_+ \Phi_{2k} = g_{2k}(\Phi_0, \Phi_1, \ldots, \Phi_{2k-1}), \quad L_- \Phi_{2k+1} = g_{2k+1}(\Phi_0, \Phi_1, \ldots, \Phi_{2k}), \quad k \in \mathbb{N}, \tag{2.10}$$

where $L_+ = -\partial_Z^2 + 1 - 6\operatorname{sech}^2(Z)$ and g_n contains linear and cubic powers of $(\Phi_0, \Phi_1, \ldots, \Phi_{n-1})$ and their derivatives up to the $(n+2)$th order that follow from the power expansions of (2.5) and (2.6). For instance,

$$\begin{aligned} g_2 = \frac{1}{12} \left(\Phi_0''''(Z) - \Phi_0(Z) \right) + \alpha \Phi_0^2(Z) \Phi_0''(Z) - \frac{2}{S^2} \Phi_1^2(Z) \Phi_0(Z) \\ + \frac{\sin(\beta)}{3\cos(\beta)} \left(\Phi_1'''(Z) - \Phi_1'(Z) + 6\alpha |\Phi_0(Z)|^2 \Phi_1'(Z) \right). \end{aligned}$$

It is easy to check that $g_{2k}(Z)$ is even on $\mathbb{R}$, while $g_{2k+1}(Z)$ is odd on $\mathbb{R}$. Since $L_+\Phi_0' = 0$ and $L_-\Phi_0 = 0$, where $\Phi_0'(Z)$ is odd on $\mathbb{R}$ and $\Phi_0(Z)$ is even on $\mathbb{R}$, respectively, there exists a unique solution of the linear inhomogeneous equations (2.10) in the space of even functions for $\Phi_{2k}(Z)$ and odd functions for $\Phi_{2k+1}(Z)$. Therefore, the asymptotic expansion for $\Phi(Z)$ can be computed up to any order of κ. However, this expansion does not capture the behavior of the oscillatory tails as their amplitude is exponentially small as $\kappa \to 0$, and hence the oscillatory tails lie beyond all orders of the asymptotic expansion. Oscillatory tails are generated by the radiation modes related to purely imaginary roots of the dispersion relation (see (3.6) below). We will perform a beyond all orders asymptotic analysis of the oscillatory tails following the algorithm described in [15] in the context of a saturable DNLS equation.

3. Beyond all orders asymptotic expansion. The radiation tail to a traveling wave may appear in the solution to the outer equation (2.4) beyond all orders of the asymptotic expansion in powers of κ. By analyzing the outer expansion near a singularity in the complex Z-plane and by rescaling dependent and independent variables with the blow-up technique [22], the amplitude of the radiation tail can be measured at the leading order approximation. The leading order term of the outer expansion, $\Phi_0(Z) = S\,\mathrm{sech}(Z)$, has its first singularity at $Z = \frac{i\pi}{2}$. Therefore, we take

$$\psi(\zeta) = \kappa\Phi(Z), \quad \theta(\zeta) = \kappa\overline{\Phi}(Z), \quad Z = \kappa\zeta + \frac{i\pi}{2}. \tag{3.1}$$

Note that because $Z \in \mathbb{C}$, it is no longer true that $\overline{\theta(\zeta)} = \psi(\zeta)$. The change of coordinates leads to the system of equations

$$\begin{aligned}
&\cos(\beta)\left[\psi(\zeta+1) + \psi(\zeta-1) - 2\cosh(\kappa)\psi(\zeta)\right] \\
&+ i\sin(\beta)\left[\psi(\zeta+1) - \psi(\zeta-1) - \frac{2\sinh(\kappa)}{\kappa}\psi'(\zeta)\right] + F(\psi,\theta) = 0, \\
&\cos(\beta)\left[\theta(\zeta+1) + \theta(\zeta-1) - 2\cosh(\kappa)\theta(\zeta)\right] \\
&- i\sin(\beta)\left[\theta(\zeta+1) - \theta(\zeta-1) - \frac{2\sinh(\kappa)}{\kappa}\theta'(\zeta)\right] + G(\psi,\theta) = 0,
\end{aligned} \tag{3.2}$$

where

$$\begin{aligned}
F &= 2(1-\alpha)\psi^2(\zeta)\theta(\zeta) + \alpha\psi(\zeta)\theta(\zeta)\left(\cos(\beta)[\psi(\zeta+1) + \psi(\zeta-1)]\right. \\
&\qquad \left. + i\sin(\beta)[\psi(\zeta+1) - \psi(\zeta-1)]\right), \\
G &= 2(1-\alpha)\psi(\zeta)\theta^2(\zeta) + \alpha\psi(\zeta)\theta(\zeta)\left(\cos(\beta)[\theta(\zeta+1) + \theta(\zeta-1)]\right. \\
&\qquad \left. - i\sin(\beta)[\theta(\zeta+1) - \theta(\zeta-1)]\right).
\end{aligned}$$

The system in the form (3.2) is said to be the inner equation for the bifurcation. This system is equivalent to the outer equation (2.4) after the transformation (3.1). Solutions to the inner equations can be expanded in powers of κ as follows:

$$\psi(\zeta) = \psi_0(\zeta) + \sum_{n=1}^{\infty}\kappa^{2n}\psi_n(\zeta), \quad \theta(\zeta) = \theta_0(\zeta) + \sum_{n=1}^{\infty}\kappa^{2n}\theta_n(\zeta). \tag{3.3}$$

Substituting (3.3) into (3.2) gives, to leading order, $O(\kappa^0)$,

$$\begin{aligned}\cos(\beta)\left[\psi_0(\zeta+1)+\psi_0(\zeta-1)-2\psi_0(\zeta)\right]+i\sin(\beta)\left[\psi_0(\zeta+1)-\psi_0(\zeta-1)-2\psi_0'(\zeta)\right]\\ +F(\psi_0,\theta_0)=0,\\ \cos(\beta)\left[\theta_0(\zeta+1)+\theta_0(\zeta-1)-2\theta_0(\zeta)\right]-i\sin(\beta)\left[\theta_0(\zeta+1)-\theta_0(\zeta-1)-2\theta_0'(\zeta)\right]\\ +G(\psi_0,\theta_0)=0.\end{aligned}$$

Note that we are interested in the limit $\kappa \to 0$, and therefore we will need to solve equations of the leading order only [22]. By continuing the inner asymptotic expansion, we formally obtain the inverse power series

$$\psi_0(\zeta)=\sum_{n=1}^{\infty}\frac{a_n}{\zeta^n},\quad \theta_0(\zeta)=\sum_{n=1}^{\infty}\frac{b_n}{\zeta^n}. \tag{3.4}$$

Substituting these inverse power series into the system of equations for ψ_0 and θ_0 gives, at leading order, $O(\zeta^{-3})$,

$$a_1S^2+a_1^2b_1=0,\quad b_1S^2+b_1^2a_1=0, \tag{3.5}$$

which has a symmetric solution $a_1 = b_1 = -iS$. This solution corresponds to the leading order term in the expansion

$$\Phi_0(Z)=S\,\mathrm{sech}(Z)=\frac{S}{i\kappa\zeta+O(\kappa^3\zeta^3)}=\frac{-iS}{\kappa\zeta}\left(1+O(\kappa^2\zeta^2)\right)$$

as $\kappa \to 0$. We shall now consider the convergence of the inverse power series (3.4). First, by substituting $\theta_0(\zeta) = e^{-p\zeta}$ into the second equation of the system with $G \equiv 0$, we define the dispersion relation in the form

$$D(p;\beta):=\cos(\beta)[\cosh(p)-1]+i\sin(\beta)[\sinh(p)-p]=0. \tag{3.6}$$

By substituting $\psi_0(\zeta) = e^{-p\zeta}$ into the first equation of the system with $F \equiv 0$, we obtain the dispersion relation in the form $\bar{D}(p;\beta) = 0$. Examining roots of $D(p;\beta)$, we can see that $p = 0$ is a triple root if $\beta = \frac{\pi}{2}$ and a double root if $\beta \neq \frac{\pi}{2}$. If $\beta = \frac{\pi}{2}$, there are no other purely imaginary roots of $D(p;\beta)$ in p. Analysis near this special point was reported in [19]; in this situation the radiation modes already appear at the algebraic order of asymptotic expansions, and no analysis of beyond all orders terms is necessary. We are interested in the existence of solutions away from this special point, when the radiation modes appear truly beyond all orders. If $\beta \neq \frac{\pi}{2}$, then $p = 0$ is a double root of $D(p;\beta)$, and there also exists a varying number of imaginary roots, $p \in i\mathbb{R}$, depending upon the value of β. If $\beta \in (0,\pi)$ (that is, $c > 0$), there are finitely many roots $p \in i\mathbb{R}$ for any value of β. Let $p = ik_0$ be the smallest root of $D(p;\beta)$ on the imaginary axis; moreover, k_0 is the only nonzero root on the imaginary axis for $\beta \in (\beta_0,\beta_1)$, where $\beta_0 \approx \frac{\pi}{13}$ and $\beta_1 \approx \frac{13\pi}{14}$; see Figure 1. A symmetric root $p = -ik_0$ exists for $\bar{D}(p;\beta)$. Owing to the resonance caused by the roots $p = \pm ik_0$, the solution to the system of inner equations could have an oscillatory tail as $|\mathrm{Re}(\zeta)| \to \infty$; therefore, we now

consider a linearization around the inverse power series for $\psi_0(\zeta)$ and $\theta_0(\zeta)$. To accommodate both cases $k_0 > 0$ and $k_0 < 0$, we write

$$\psi_0(\zeta) = \frac{-iS}{\zeta} + \Gamma\hat{\psi}(\zeta)e^{-i|k_0|\zeta} + \sum_{n=2}^{\infty}\frac{a_n}{\zeta^n}, \quad \theta_0(\zeta) = \frac{-iS}{\zeta} + \Gamma\hat{\theta}(\zeta)e^{-i|k_0|\zeta} + \sum_{n=2}^{\infty}\frac{b_n}{\zeta^n}, \tag{3.7}$$

where the exponential term $e^{-i|k_0|\zeta} = e^{-\frac{\pi|k_0|}{2\kappa}}e^{-\frac{ik_0Z}{\kappa}}$ describes the beyond all orders effects due to the coefficient set $e^{-\frac{\pi|k_0|}{2\kappa}}$ becoming exponentially small in the limit $\kappa \to 0^+$. The coefficient Γ is a measure of the amplitude of the oscillatory tail so that a localized solution exists only if $\Gamma = 0$. Substituting (3.7) into the system of inner equations at the leading order and truncating the nonlinear terms to $O(\zeta^{-3})$ gives a linearized system for $\hat{\psi}(\zeta)$ and $\hat{\theta}(\zeta)$ in the form

$$\begin{aligned}
&\cos(\beta)\left[\hat{\psi}(\zeta+1)e^{-i|k_0|} + \hat{\psi}(\zeta-1)e^{i|k_0|} - 2\hat{\psi}(\zeta)\right]\left(1-\frac{\alpha S^2}{\zeta^2}\right)\\
&+ i\sin(\beta)\left[\left(\hat{\psi}(\zeta+1)e^{-i|k_0|} - \hat{\psi}(\zeta-1)e^{i|k_0|}\right)\left(1-\frac{\alpha S^2}{\zeta^2}\right) - 2\hat{\psi}'(\zeta) + 2i|k_0|\hat{\psi}(\zeta)\right]\\
&- \frac{2\cos(\beta)}{\zeta^2}\left(2\hat{\psi}(\zeta) + \hat{\theta}(\zeta)\right) + \mathrm{O}(\zeta^{-3}) = 0,\\
&\cos(\beta)\left[\hat{\theta}(\zeta+1)e^{-i|k_0|} + \hat{\theta}(\zeta-1)e^{i|k_0|} - 2\hat{\theta}(\zeta)\right]\left(1-\frac{\alpha S^2}{\zeta^2}\right)\\
&- i\sin(\beta)\left[\left(\hat{\theta}(\zeta+1)e^{-i|k_0|} - \hat{\theta}(\zeta-1)e^{i|k_0|}\right)\left(1-\frac{\alpha S^2}{\zeta^2}\right) - 2\hat{\theta}'(\zeta) + 2i|k_0|\hat{\theta}(\zeta)\right]\\
&- \frac{2\cos(\beta)}{\zeta^2}\left(2\hat{\theta}(\zeta) + \hat{\psi}(\zeta)\right) + \mathrm{O}(\zeta^{-3}) = 0.
\end{aligned} \tag{3.8}$$

Using a Laurent expansion for $\hat{\psi}(\zeta)$ and $\hat{\theta}(\zeta)$ with some integer exponent r, yet to be determined,

$$\begin{aligned}
\hat{\psi}(\zeta) &= \rho_1\zeta^r + \rho_2\zeta^{r-1} + \rho_3\zeta^{r-2} + O(\zeta^{r-3}),\\
\hat{\theta}(\zeta) &= \eta_1\zeta^r + \eta_2\zeta^{r-1} + \eta_3\zeta^{r-2} + O(\zeta^{r-3}),
\end{aligned}$$

the linearized system (3.8) can be solved at each successive power of r, giving for the $\hat{\psi}(\zeta)$ equation

$$\begin{aligned}
O(\zeta^r) \quad & \rho_1 D(-i|k_0|;\beta) = 0,\\
O(\zeta^{r-1}) \quad & \rho_2 D(-i|k_0|;\beta) + \rho_1 r D'(-i|k_0|;\beta) = 0,\\
O(\zeta^{r-2}) \quad & \rho_3 D(-i|k_0|;\beta) + \rho_2(r-1)D'(-i|k_0|;\beta) + \rho_1\frac{r(r-1)}{2}D''(-i|k_0|;\beta)\\
& - \cos(\beta)(2\rho_1+\eta_1) - \sin(\beta)\alpha S^2|k_0|\rho_1 = 0
\end{aligned}$$

and for the $\hat{\theta}(\zeta)$ equation

$$
\begin{aligned}
O(\zeta^r) \quad & \eta_1 D(i|k_0|;\beta) = 0,\\
O(\zeta^{r-1}) \quad & \eta_2 D(i|k_0|;\beta) + \eta_1 r D'(i|k_0|;\beta) = 0,\\
O(\zeta^{r-2}) \quad & \eta_3 D(i|k_0|;\beta) + \eta_2 (r-1) D'(i|k_0|;\beta) + \eta_1 \frac{r(r-1)}{2} D''(i|k_0|;\beta)\\
& - \cos(\beta)\,(2\eta_1 + \rho_1) + \sin(\beta)\alpha S^2 |k_0| \eta_1 = 0,
\end{aligned}
$$

where derivatives of $D(p;\beta)$ are taken with respect to p at $p = \pm i|k_0|$. If $\beta < \frac{\pi}{2}$, then $k_0 > 0$ and $p = ik_0$ is a root of $D(p;\beta)$ but not a root of $\bar{D}(p;\beta)$. Therefore, $D(i|k_0|;\beta) = 0$ and $D(-i|k_0|;\beta) \neq 0$ for $\beta < \frac{\pi}{2}$. To avoid the trivial solution, we normalize $\eta_1 = 1$. Since $D'(i|k_0|;\beta) \neq 0$, we find $r = 0$ and obtain unique values for the coefficients of the power series, e.g.,

(3.9)

$$
\rho_1 = 0, \quad \rho_2 = 0, \quad \rho_3 = \frac{\cos(\beta)}{D(-i|k_0|;\beta)}, \ldots, \quad \eta_1 = 1, \quad \eta_2 = \frac{-2\cos(\beta) + \sin(\beta)\alpha S^2 |k_0|}{D'(i|k_0|;\beta)}, \ldots.
$$

The solution so far is

(3.10)

$$
\begin{aligned}
\psi_0(\zeta) &= \frac{-iS}{\zeta} + \Gamma \left[\frac{\cos(\beta)}{D(-i|k_0|;\beta)} \frac{1}{\zeta^2} + O\left(\frac{1}{\zeta^3}\right) \right] e^{-i|k_0|\zeta} + \sum_{n=2}^{\infty} \frac{a_n}{\zeta^n},\\
\theta_0(\zeta) &= \frac{-iS}{\zeta} + \Gamma \left[1 + \frac{-2\cos(\beta) + \sin(\beta)\alpha S^2 |k_0|}{D'(i|k_0|;\beta)} \frac{1}{\zeta} + O\left(\frac{1}{\zeta^2}\right) \right] e^{-i|k_0|\zeta} + \sum_{n=2}^{\infty} \frac{b_n}{\zeta^n}.
\end{aligned}
$$

If $\beta > \frac{\pi}{2}$, then $k_0 < 0$, such that $D(-i|k_0|;\beta) = 0$ and $D(i|k_0|;\beta) \neq 0$. As a result, the role of components $\hat{\psi}(\zeta)$ and $\hat{\theta}(\zeta)$ is swapped, compared to the previous solution (3.9)–(3.10) for $\beta < \frac{\pi}{2}$. We will develop explicit formalism for the case $\beta < \frac{\pi}{2}$, leaving the other case as an exercise for the reader.

The system of inner equations for $\psi_0(\zeta)$ and $\theta_0(\zeta)$ can be reformulated as a system of integral equations using the Borel–Laplace transform [22]:

$$
\psi_0(\zeta) = \int_\gamma V(p) e^{-p\zeta} dp, \quad \theta_0(\zeta) = \int_\gamma W(p) e^{-p\zeta} dp, \tag{3.11}
$$

which gives

$$
\begin{aligned}
&\overline{D}(p;\beta) V + V * W * \left(\left[(1-\alpha) + \alpha\cos(\beta)\cosh(p) - i\alpha\sin(\beta)\sinh(p) \right] V \right) = 0,\\
&D(p;\beta) W + W * V * \left(\left[(1-\alpha) + \alpha\cos(\beta)\cosh(p) + i\alpha\sin(\beta)\sinh(p) \right] W \right) = 0.
\end{aligned} \tag{3.12}
$$

Here the star represents the convolution operator defined by

$$
(V * W)(p) = \int_0^p V(p - p_1) W(p_1) dp_1, \tag{3.13}
$$

where the integration is performed along a curve from the origin to the point p in the complex plane. Now consider two solutions $\{\psi_0^s(\zeta), \theta_0^s(\zeta)\}$ and $\{\psi_0^u(\zeta), \theta_0^u(\zeta)\}$ which lie on the stable and unstable manifolds, respectively, such that

$$
\begin{aligned}
\lim_{\mathrm{Re}(\zeta)\to+\infty} \psi_0^s(\zeta) &= \lim_{\mathrm{Re}(\zeta)\to+\infty} \theta_0^s(\zeta) = 0,\\
\lim_{\mathrm{Re}(\zeta)\to-\infty} \psi_0^u(\zeta) &= \lim_{\mathrm{Re}(\zeta)\to-\infty} \theta_0^u(\zeta) = 0.
\end{aligned} \tag{3.14}
$$

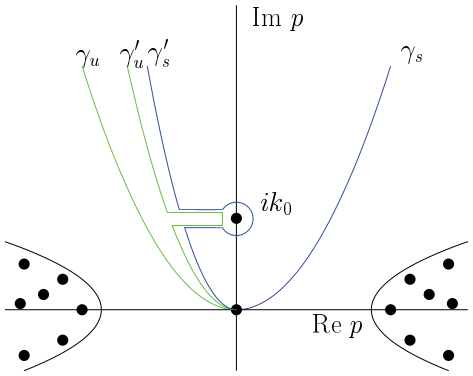

Figure 3. *Integration contours, γ, around the root ik_0, where dots indicate roots of $D(p;\beta)$.*

If a homoclinic orbit exists, then the two solutions $\{\psi_0^s(\zeta), \theta_0^s(\zeta)\}$ and $\{\psi_0^u(\zeta), \theta_0^u(\zeta)\}$ coincide. The Borel–Laplace transform (3.11) generates the solution on the stable manifold when the contour of integration $\gamma = \gamma_s$ lies in the first quadrant of the complex p-plane and produces the solution on the unstable manifold if $\gamma = \gamma_u$ lies in the second quadrant. If there are no singularities between the two integration contours γ_s and γ_u and $\{V(p), W(p)\}$ are uniformly bounded as $|p| \to \infty$ in the upper half-plane $\mathrm{Im}(p) > 0$, then the contours could be continuously deformed into each other, implying that the solution generated by each contour is the same, i.e., $\psi_0^s(\zeta) = \psi_0^u(\zeta)$ and $\theta_0^s(\zeta) = \theta_0^u(\zeta)$; therefore, the amplitude of the oscillatory tail Γ would be zero and a localized traveling wave would exist. However, as mentioned previously, there is at least one resonance $p = i|k_0|$ on the positive imaginary axis (we ignore the singularities which have $\mathrm{Re}(p) \neq 0$ as these singularities are bounded away from $\mathrm{Re}(p) = 0$, and it is hence possible to define γ_s and γ_u to lie above these points), and so deformation of the integration contours leads to a residue contribution around the singularity at $p = i|k_0|$; see Figure 3. Apart from the double root at $p = 0$, $p = ik_0$ is the only root on the positive imaginary axis for $\beta_0 < \beta < \beta_1$, and all other roots are bounded away from $\mathrm{Re}(p) = 0$.

Let us now put into correspondence the behavior of the leading order terms $\psi_0(\zeta)$ and $\theta_0(\zeta)$ as given by (3.10) and the poles of $V(p)$ and $W(p)$. To generate the expansion (3.10), the functions $V(p)$ and $W(p)$ must be of the form

$$
\begin{aligned}
V(p) &= O\left((p - i|k_0|)\log(p - i|k_0|)\right) - iS + \sum_{n=2}^{\infty} a_n p^{n-1}, \\
W(p) &= \frac{\Gamma}{2\pi i(p - i|k_0|)} + O(\log(p - i|k_0|)) - iS + \sum_{n=2}^{\infty} b_n p^{n-1},
\end{aligned}
\tag{3.15}
$$

where the pole term arises from the term $e^{-i|k_0|\zeta}$, the logarithmic terms arise from the terms $\zeta^{-m}e^{-i|k_0|\zeta}$ with $m \geq 1$, and the power terms arise from the inverse power terms ζ^{-m} with $m \geq 1$. The constant Γ is referred to as the Stokes constant. Only if the constant Γ is zero may there exist a homoclinic orbit to the rest state, and therefore there may exist a localized traveling wave. All other singular terms in the expansion (3.15) are subordinate to the simple pole with the residue coefficient Γ. The inverse power series in ζ for $\psi_0(\zeta)$ and $\theta_0(\zeta)$ given by

(3.4) become the power series expansions in p for $V(p)$ and $W(p)$,

$$V(p) = \sum_{n=0}^{\infty} V_n p^n, \quad W(p) = \sum_{n=0}^{\infty} W_n p^n. \tag{3.16}$$

Since no singularities are present in the neighborhood of the origin $p = 0$, the power series (3.16) converge near the origin but diverge as $p \to i|k_0|$, where they should recover the pole singularity of the solution (3.15), according to the matching condition

$$\sum_{n=0}^{\infty} W_n p^n \xrightarrow[p \to i|k_0|]{} \frac{\Gamma}{2\pi|k_0|} \frac{1}{1 + \frac{ip}{|k_0|}} = \frac{\Gamma}{2\pi|k_0|} \sum_{n=0}^{\infty} \frac{(-ip)^n}{|k_0|^n}. \tag{3.17}$$

The Stokes constant is hence given by

$$\Gamma = 2\pi|k_0| \lim_{n\to\infty} (i|k_0|)^n W_n. \tag{3.18}$$

We shall use this formula for numerical computation of the Stokes constant in the following section.

4. Computation of the Stokes constant. We will now compute the Stokes constant by computing the limit (3.18). Since we consider power series solutions (3.16) of the system of integral equations (3.12), we expand the dispersion relation $D(p;\beta)$ as a power series

$$D(p;\beta) = \cos(\beta) \sum_{n=1}^{\infty} \frac{p^{2n}}{(2n)!} + i \sin(\beta) \sum_{n=1}^{\infty} \frac{p^{2n+1}}{(2n+1)!}. \tag{4.1}$$

The convolution operator for power series solutions (3.16) becomes

$$(V * W)(p) = \sum_{n_1=0}^{\infty} \sum_{n_2=0}^{\infty} \frac{n_1! n_2!}{(n_1 + n_2 + 1)!} V_{n_1} W_{n_2} p^{n_1+n_2+1}. \tag{4.2}$$

Substituting (3.16), (4.1), and (4.2) into system (3.12) gives a power series in p that can be solved for each value of n to give coefficients (V_n, W_n) in terms of the preceding coefficients $\{(V_m, W_m),\ 0 \le m < n\}$. The first two terms of the power series (3.16) are

$$\begin{aligned} n = 2 &\to V_0 = W_0 = -iS, \\ n = 3 &\to V_1 = -W_1 = \frac{\sin(\beta) S^3 (1-\alpha)}{2\cos^2(\beta)}. \end{aligned}$$

Obtaining a good approximation for coefficients V_n and W_n, when n is large, is computationally difficult owing to V_n and W_n becoming either very large or very small in the large n limit. To improve the performance of the numerical computations, it is advantageous to normalize the coefficients by using the limit (3.18). Since the symmetry of equations implies that $W(p) = V(-p)$ (see [15]), we use the substitution

$$V_n = \frac{-i(-1)^n \tau_n}{(i|k_0|)^n}, \quad W_n = \frac{-i\tau_n}{(i|k_0|)^n}, \quad n \in \mathbb{N}, \tag{4.3}$$

with $\tau_0 = S$ and $\tau_1 = \frac{\sin(\beta)S^3(1-\alpha)|k_0|}{2\cos^2(\beta)}$, and convert the system of integral equations (3.12) into a scalar recurrence equation for the unknown real-valued coefficients τ_n. The Stokes constant, denoted finally by $K(\alpha;\beta)$, is now given by

$$K(\alpha;\beta) \equiv i\Gamma = 2\pi|k_0| \lim_{n\to\infty} \tau_n. \tag{4.4}$$

We note that this formula is valid for $\beta < \frac{\pi}{2}$, when the pole singularity occurs in the component $W(p)$ in (3.10). If $\beta > \frac{\pi}{2}$, the pole singularity occurs in the component $V(p)$, as per previous discussion. However, because of the relation $W(p) = V(-p)$, the same substitution (4.3) can be used with a modified definition of the Stokes constant $K(\alpha;\beta) = 2\pi|k_0| \lim_{n\to\infty}(-1)^n\tau_n = 2\pi|k_0| \lim_{n\to\infty}|\tau_n|$ for both $\beta < \frac{\pi}{2}$ and $\beta > \frac{\pi}{2}$.

At each value of n, the recurrence equation for τ_n in terms of the coefficients $(\tau_0, \ldots, \tau_{n-1})$ is a linear equation of the form

$$\cos(\beta)\left(\frac{1}{2} - \frac{(2+(-1)^n)}{(n+2)(n+1)}\right)\tau_n = Q_n(\tau_0, \tau_1 \ldots \tau_{n-1}), \tag{4.5}$$

where Q_n is uniquely defined for each $n \geq 1$. It is clear that (4.5) is nonsingular for all $n \geq 1$ provided that $\cos(\beta) \neq 0$ (that is, $\beta \neq \frac{\pi}{2}$). We shall consider the Stokes constant only for $\beta \in (\beta_0, \frac{\pi}{2}) \cup (\frac{\pi}{2}, \beta_1)$, since for $\beta < \beta_0$ and $\beta > \beta_1$ the pair $p = \pm ik_0$ does not give all roots of the dispersion relation on the imaginary axis. As a result, finding a simple zero of $K(\alpha;\beta)$ for $\beta < \beta_0$ and $\beta > \beta_1$ is not sufficient for predicting bifurcations of a truly localized solution as we would also have to compute the Stokes constants for other radiation modes corresponding to other eigenvalues on the imaginary axis.

In the case of the AL lattice ($\alpha = 1$), there exists an explicit traveling wave solution for all values of β, and, as mentioned in section 2, this solution is captured by the first term of the asymptotic expansion, $\Phi_0(Z) = \mathrm{sech}(Z)$. Therefore, we would expect that $K(1;\beta) \equiv 0$ for all β. Setting $\alpha = 1$ gives $\tau_0 = S = 1$ and $\tau_1 = 0$. If we assume that $\tau_1 = \tau_2 = \cdots = \tau_{n-1} = 0$, then a direct computation shows that τ_n is given by

$$\cos(\beta)\left(\frac{1}{2} - \frac{(2+(-1)^n)}{(n+2)(n+1)}\right)\tau_n = \begin{cases} \frac{(i|k_0|)^n}{(n+2)!}\tau_0\cos(\beta)(1-\tau_0^2) & \text{if } n \text{ is even,} \\ \frac{-|k_0|(i|k_0|)^{n-1}}{(n+2)!}\tau_0\sin(\beta)(1-\tau_0^2) & \text{if } n \text{ is odd.} \end{cases} \tag{4.6}$$

Since for $\alpha = 1$, $\tau_0 = 1$, then the right-hand side of (4.6) is equal to 0, and so $\tau_n = 0$ if $\tau_1 = \cdots = \tau_{n-1} = 0$. Therefore, indeed $K(1;\beta) \equiv 0$ for all values of β.

Equation (4.5) is computed numerically for a large value of n for fixed values of parameters (α, β) giving a good approximation to the Stokes constant. We are interested in the behavior of $K(\alpha;\beta)$ as α and β are varied. First, let us consider the two limiting cases: the cubic DNLS model with $\alpha = 0$, where we expect the Stokes constant to be nonzero for all β, and the integrable AL model with $\alpha = 1$, where we have shown that $\tau_n = 0$ for all $n \geq 1$. These two models will give us a good check on the validity of the numerical code and are shown in Figure 4. The results agree with our predictions. Indeed, results of [15, 19] show that no single-humped localized traveling waves exist in the cubic DNLS model, while a two-parameter family of traveling wave solutions is known for the AL model.

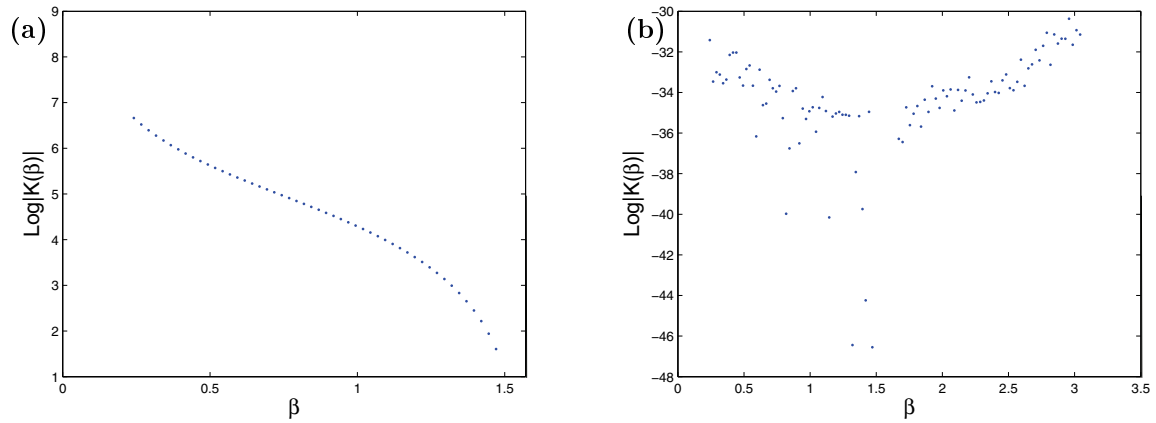

Figure 4. *Computation of the Stokes constant $K(\alpha;\beta)$ for* (a) *cubic DNLS, $\alpha = 0$, and* (b) *AL model, $\alpha = 1$. There are no zeros of the Stokes constant for the cubic DNLS, while the Stokes constant for the AL model is always zero (to numerical round-off).*

Now we consider the intermediate values $\alpha \in (0,1)$. If $\alpha < 0.5$, then Figure 2 suggests that the computations must be restricted to the domain $\beta \in (\beta_0, \pi/2)$. Figures 5 (a)–(b) show that no zeros of $K(\beta)$ are found for $\alpha \in [0, 0.5]$. If $\alpha > 0.5$, computations are extended to the domain $\beta \in (\beta_0, \pi/2) \cup (\beta_*, \beta_1)$. A number of zeros of $K(\beta)$ are found in the second interval (β_*, β_1), as is shown in Figures 5 (c)–(d). The number of zeros of $K(\alpha;\beta)$ depends on the value of α, and each zero moves toward the point $\beta = \pi/2$ as $\alpha \to 1$. The existence of at least one traveling wave solution for $\beta > \pi/2$ agrees with the preliminary results in [18], where a traveling wave was found numerically for $\alpha = 0.7$ and $\beta = 0.875\pi$.

5. Numerical computation of traveling waves. The existence of a zero of the Stokes constant $K(\alpha;\beta)$ predicts a possible bifurcation of a traveling soliton, so we confirm here this prediction by finding localized solutions to the differential advance-delay equation (2.4). In addition, we test the stability of localized solutions by direct numerical integration of the DNLS equation (1.1).

5.1. Localized solutions of the differential advance-delay equation. To find localized solutions to the differential advance-delay equation (2.4) and to continue them as parameters vary, we use the method we have developed in earlier papers [13, 14, 18] based upon the earlier work of [2, 6, 7]. Specifically, a pseudospectral method is used to compute a numerical solution by extending $\Phi(Z)$ into a periodic function over a large finite domain $(-L/2, L/2)$,

$$\Phi(Z_i) = \sum_{j=0}^{N+1} a_j \cos\left(\frac{2\pi j}{L} Z_i\right) + i b_j \sin\left(\frac{2\pi j}{L} Z_i\right). \tag{5.1}$$

The differential advance-delay equation (2.4) is then decomposed into a large system of $2N+2$ algebraic equations posed on the collocation points $Z_i = \frac{Li}{2(N+1)}$ for $-(N+1) \le i \le (N+1)$ with the periodic boundary conditions $\Phi(Z_{N+1}) = \Phi(Z_{-(N+1)})$. This system is solved by using a Powell hybrid method [20], and a localized solution, if it exists, is continued numerically in parameter space using AUTO [5]. By using an appropriate signed measure of the radiation

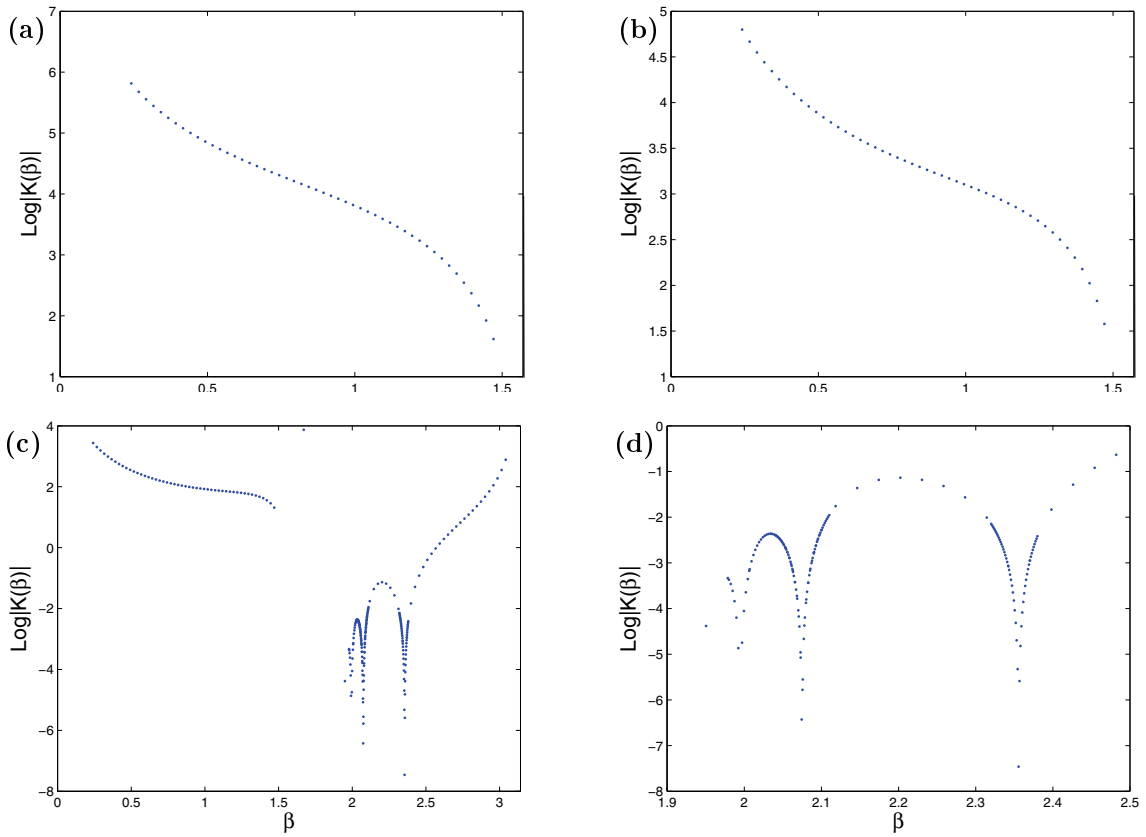

Figure 5. *Computation of the Stokes constant $K(\alpha;\beta)$ for the Salerno model with varying β for $\alpha = 0.25$* (a)*, $\alpha = 0.5$* (b)*, and $\alpha = 0.75$* (c)*. The zoomed graph* (d) *shows that zeros of $K(\alpha;\beta)$ exist at $\beta \approx 1.98, 2.08, 2.36$ for $\alpha = 0.75$.*

tail amplitude, $\Delta = \mathrm{Im}(\Phi(L/2))$, based upon the symmetry of the periodic function, traveling localized solutions can be found as regular zeros of Δ; see [14]. Figures 6 (a)–(b) show the correspondence between zeros of the Stokes constant $K(\alpha;\beta)$, where there are four distinct zeros for $\kappa = 0$, and zeros of Δ, where there are two zeros for $\kappa = 0.5$, in the case $\alpha = 0.65$. The discrepancy in the number of zeros between the Stokes constant calculations and the pseudospectral computations is related to the fact that the number of branches for a fixed α changes when κ increases.

We would expect the zeros of Δ to approach the zeros of $K(\alpha;\beta)$ as κ is reduced toward zero. However, since κ is a measure of the amplitude and width of the localized solution, continuing the solutions of the differential advance-delay equation (2.4) for small κ is a problematic computation as the solution becomes broad and has a small amplitude in this limit. It is a much easier task to compute continuation curves for a fixed nonzero value of κ in the (α,β)-plane and reduce the value of κ. Such continuations for nonzero κ are shown in Figure 7 (a). Three curves of $\Delta = 0$ for $\kappa = 0.3, 0.5, 1$ are also shown. These curves approach the line $K(\alpha;\beta) = 0$ for $\beta > \frac{\pi}{2}$ as κ becomes smaller. All existence curves have a fold point at the maximum value of α for some value of $\beta < \frac{\pi}{2}$, which approaches the point $(\alpha,\beta) = \left(1, \frac{\pi}{2}\right)$

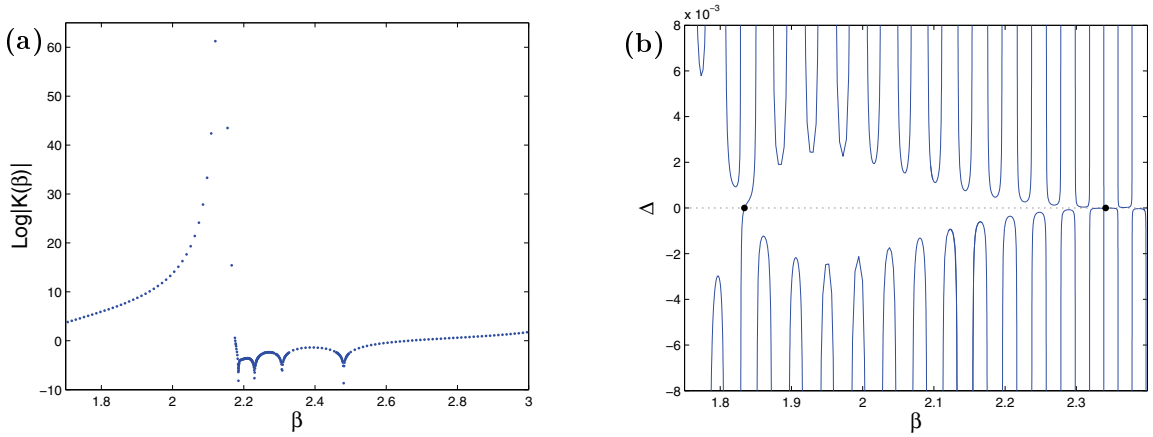

Figure 6. *Existence of traveling wave solutions in the Salerno model for $\alpha = 0.65$ computed via calculation of* (a) *the Stokes constant $K(\alpha;\beta)$ ($\kappa = 0$) and* (b) *the radiation tail amplitude Δ ($\kappa = 0.5$). A number of points where localized waves exist are found, at $\beta \approx 2.182$, 2.237, 2.308, and 2.48, using the Stokes constant method, and at $\beta \approx 1.834, 2.340$, using the radiation tail amplitude (indicated by dots).*

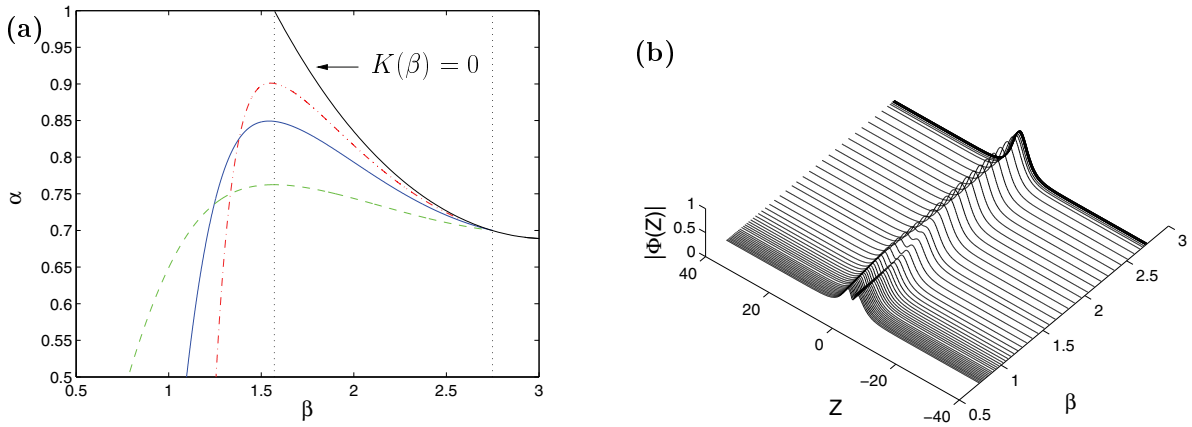

Figure 7. (a) *Continuation of numerical solutions to the differential advance-delay equation (2.4) for varying α and β with $\kappa = 0.3$ (dash-dot line), $\kappa = 0.5$ (solid line), and $\kappa = 1$ (dashed line). As β is reduced, a fold bifurcation occurs and the single-humped solution splits into a double-humped one. Continuation of the first (highest β) zero of the Stokes constant $K(\alpha;\beta)$ is shown as a solid black line. Dotted vertical lines indicate the special points $\beta = \pi/2$ and $\beta = \beta_1$.* (b) *Profiles $|\Phi(Z)|$ along the continuation branch with $\kappa = 0.5$ showing the splitting of single-humped solutions into double-humped ones.*

as $\kappa \to 0$. For β less than this fold point the solutions split into double-humped solutions, as shown in panel (b).

Figure 8 illustrates the correspondence between subsequent zeros of $K(\alpha;\beta)$ shown by solid lines and zeros of Δ shown by dashed lines for $\kappa = 0.5$. As in the previous case, all the lines of $K(\alpha;\beta) = 0$ seem to originate from the point $(\alpha,\beta) = (1, \frac{\pi}{2})$, and the numerical approximations to solutions obtained using the pseudospectral method match up well with the lines of $K(\alpha;\beta) = 0$ for $\beta > \frac{\pi}{2}$. In contrast, for $\beta < \frac{\pi}{2}$ the branches experience a fold with respect to α, and the corresponding single-humped solutions become multihumped solutions

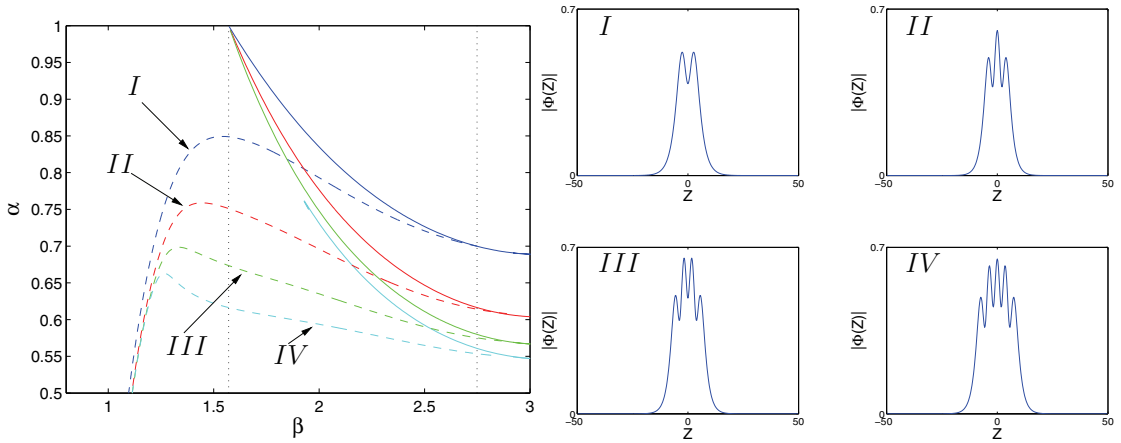

Figure 8. *Continuation of zeros of the Stokes constants (solid lines) along with the corresponding branches of solutions with zero radiation tail $\Delta = 0$ for $\kappa = 0.5$ (dashed lines). For $\beta < \pi/2$ the solutions are multi-humped. The number of humps corresponding to each branch* (I)–(IV) *is shown in the right panel, with $\alpha = 0.5$ for all plots and $\beta = 1.327$* (I)*, $\beta = 1.206$* (II)*, $\beta = 1.217$* (III)*, and $\beta = 1.175$* (IV)*.*

as β is decreased. The number of humps on each branch is shown in Figure 8 (right panel). The number of humps increases as α is decreased for a fixed value of β. We emphasize that all curves of $K(\alpha;\beta) = 0$ in the figure are located in the domain $\beta > \beta^*(\alpha)$, where Φ_0 is real-valued.

Figures 7 and 8 serve as an illustration of two analytical results from [18, 19]. First, the branches of single-humped solutions for $\beta > \frac{\pi}{2}$ terminate for values of $\alpha > 0.5$ away from the cubic DNLS limit $\alpha \to 0$, while the branches of multihumped solutions for $\beta < \frac{\pi}{2}$ extend to the cubic DNLS limit. Indeed, analysis of center manifold reductions near the point $\beta = \frac{\pi}{2}$ for the cubic DNLS model $\alpha = 0$ in [19] predicted an infinite number of branches of double-humped solutions and no single-humped solutions. On the other hand, both figures suggest that all solution branches for fixed values of κ have a fold point for $\alpha < 1$ away from the integrable AL limit $\alpha \to 1$. Indeed, by examining an appropriate Melnikov integral near the point $\beta = \frac{\pi}{2}$ it was found in [18] that the AL solutions do not persist for $\alpha \neq 1$ with a fixed value of $\kappa > 0$.

Figure 9 (a) is a sketch of the four solution "sheets" in $(\kappa, 1-\alpha, \beta)$-space with solutions from each sheet in panels (b)–(i). When $\kappa = 0$, only the single-humped solutions for $\beta > \frac{\pi}{2}$ and $\alpha > 0.5$ exist, corresponding to the upper parts of the sheets, but as soon as κ is nonzero, an extra branch of multihumped solutions for $\beta < \frac{\pi}{2}$ forms, corresponding to the lower parts of the sheets. The fold point joining these two branches moves in the negative direction along the (α, β)-plane, such that the only time the sheet of solutions approaches the point of the integrable AL model ($\alpha = 1$) is at $\kappa = 0$, $\beta = \frac{\pi}{2}$. Behind the sheet of solutions shown, in the negative α direction, a number of other solution sheets exist, and they correspond to the other solutions not shown in Figure 8. These solutions would be separate from all other sheets except at the point $(\alpha, \beta, \kappa) = (1, \frac{\pi}{2}, 0)$, although the multihumped sheets become close to each other for $1 - \alpha$ sufficiently large and appear to merge on the line $\beta = \frac{\pi}{2}$ as $\kappa \to 0$.

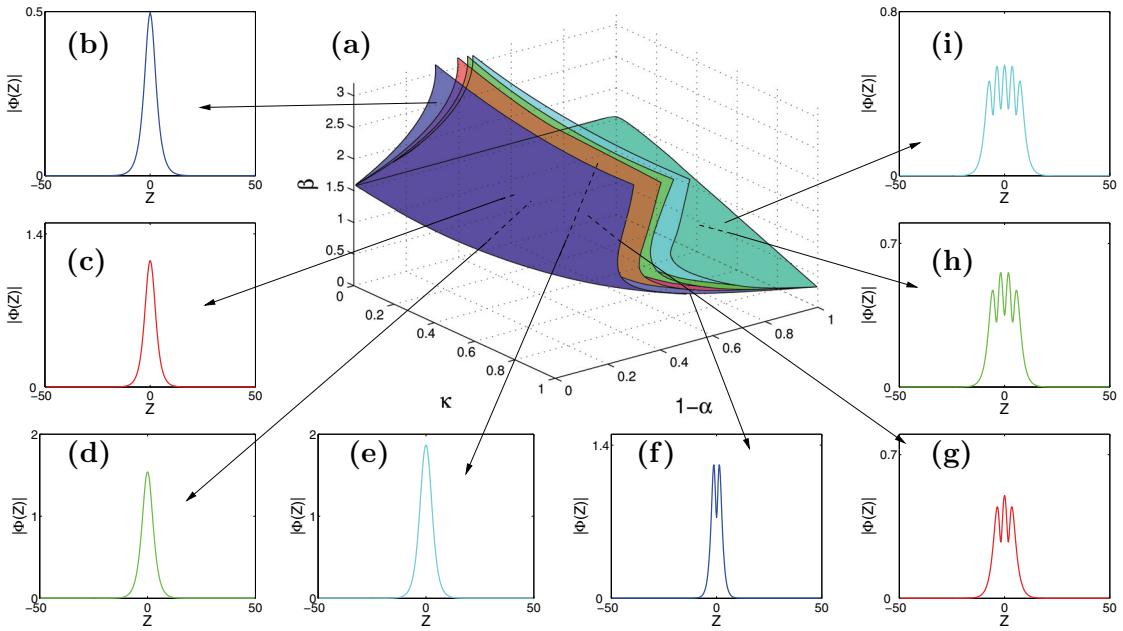

Figure 9. (a) *Existence sketch of the first four "sheets" of solutions in* $(\kappa, 1-\alpha, \beta)$*-parameter space.* (b)–(i) *Profiles of solutions from different sheets showing single-humped solutions* (b)–(e) *for the upper surfaces and multihumped solutions* (f)–(i) *on the lower surface. Colors on plots* (b)–(i) *match the solution sheet they originate from, as shown in Figure* 8.

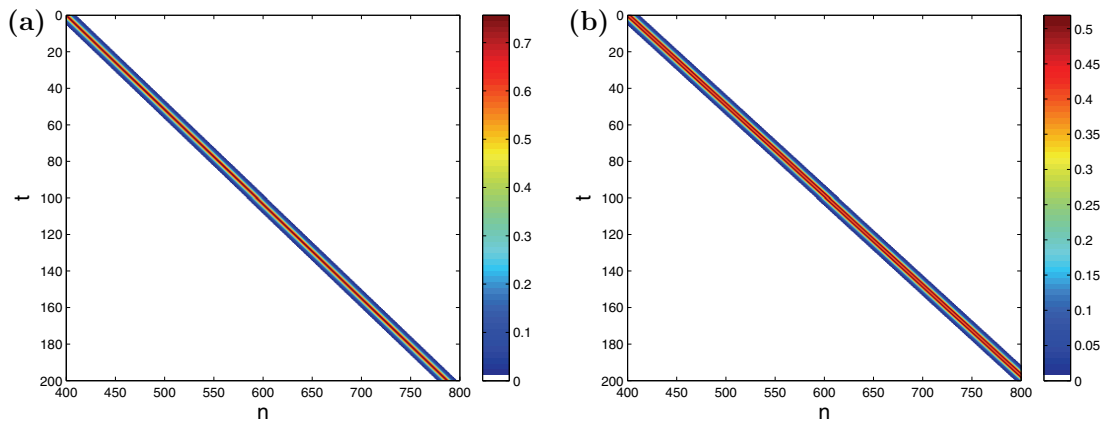

Figure 10. *Direct integration of* (a) *single-humped and* (b) *double-humped solutions to the Salerno model for* $\alpha = 0.8$, $\kappa = 0.5$ *and* (a) $\beta = 1.959$, (b) $\beta = 1.327$. *Colored regions indicate amplitudes significantly different from zero.*

5.2. Numerical integration of the DNLS equation. To simulate the single- and multihumped solutions found previously in the initial-value problem associated with the DNLS equation (1.1), we use $h = 1$ and $u_n(0) = \kappa\Phi(\kappa n)e^{i\beta n}$. Figure 10 shows the simulation of the single- and double-humped solutions for $\kappa = 0.5$ and $\alpha = 0.8$ across a lattice of $N = 800$ sites centered initially on site $n = 400$, where in all plots colored areas signify nonzero ampli-

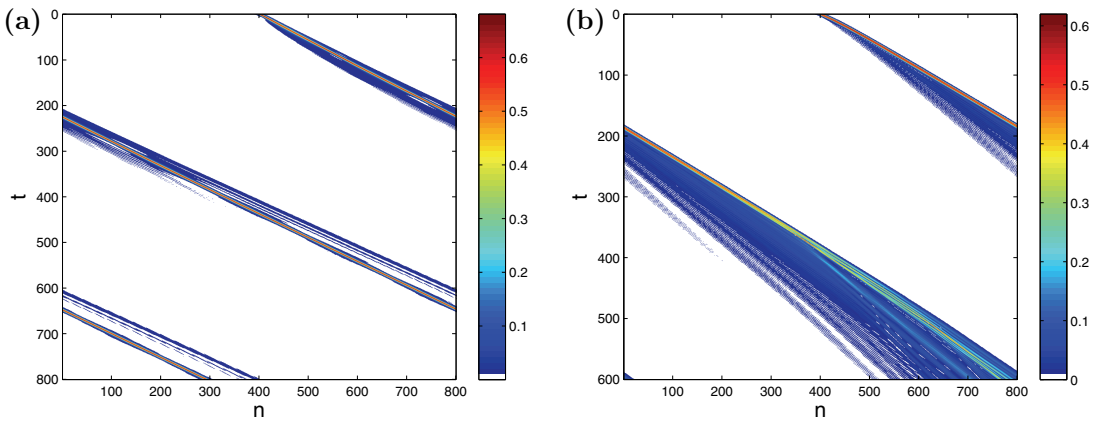

Figure 11. *Direct integration of* (a) *the single-humped solution with* $\alpha = 0.65$, $\kappa = 0.5$, $\beta = 1.834$, *and* $\mu = 0.9$; (b) *the multihumped solution with* $\alpha = 0.8$, $\kappa = 0.5$, $\beta = 1.327$, *and* $\mu = 1.1$. *Qualitatively similar results are seen for single-humped and multihumped solutions from all other branches.*

tudes. It can be seen that the solitary waves remain localized throughout the duration of the simulation.

The stability of the solitary waves can be investigated by introducing a perturbation to the initial profile of the form $\mu u_n(0)$, where $u_n(0)$ is the unperturbed initial profile and $\mu \neq 1$. Figure 11 shows the motion of a perturbed single-humped solution from branch III with $\mu = 0.9$ (panel (a)) and a perturbed double-humped solution from branch I with $\mu = 1.1$ (panel (b)). After an initial (potentially long) transient period, where excess radiation is shed, a perturbed single-humped solution continues moving through the lattice without any more appreciable radiative losses (at least for a finite amount of time); see panel (a). In contrast, a perturbed multihumped solution continuously emits radiation across the lattice until it is no longer localized (panel (b)). Although only one example of the evolution of perturbed single- and multihumped solutions is shown in Figure 11, we note that qualitatively similar results are observed for all other branches, with the single-humped solutions appearing stable and the multihumped solutions unstable.

Collisions between localized modes in discrete lattices were exploited numerically in the context of the DNLS equation [16] and the perturbed AL equation [4]. We report here collision between two traveling wave solutions of the Salerno model. Figure 12 shows a symmetric collision between a single-humped solution and its reflected image. The collision is seen to be highly elastic with the motion of the solitons almost unaffected by the collision, although there is a slight variation in the amplitude of the solitons after the collision. An asymmetric collision between a single-humped solution and a reflected multihumped solution is shown in Figure 13. Here the effect of the collision is much greater with the multihumped solution (traveling in the negative n direction) exhibiting a slowly decaying amplitude while the single-humped solution exhibits a rapidly varying amplitude.

6. Conclusion. We have analyzed the existence of localized traveling waves (homoclinic orbits to the rest state) in the Salerno model by computing zeros of the Stokes constant and homoclinic orbits of the differential advance-delay equation. Branches of zeros of the

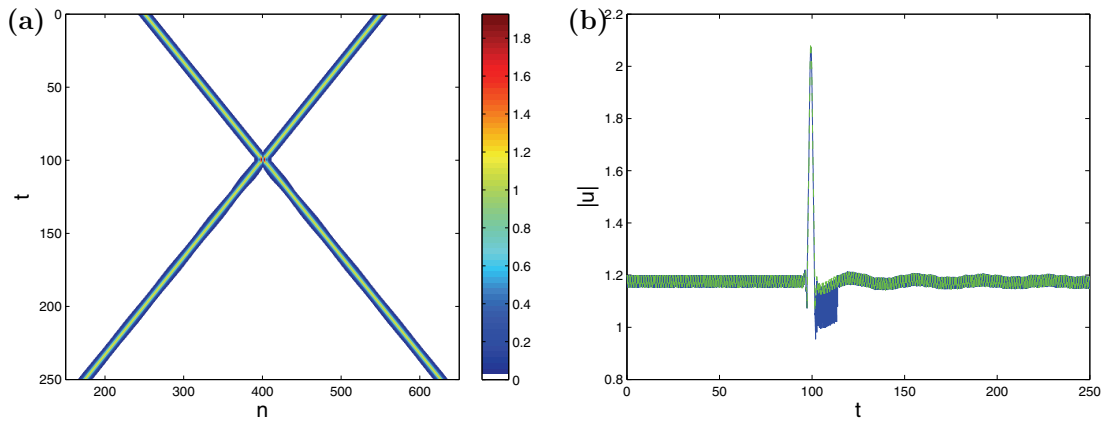

Figure 12. (a) *Collision between a single-humped solution from branch* II *and its reflected image for* $\alpha = 0.65$ *and* $\kappa = 0.5$ *across a lattice for* 250 *time steps.* (b) *Amplitudes of each traveling wave as a function of time. The collision between the traveling waves appears to be nearly elastic.*

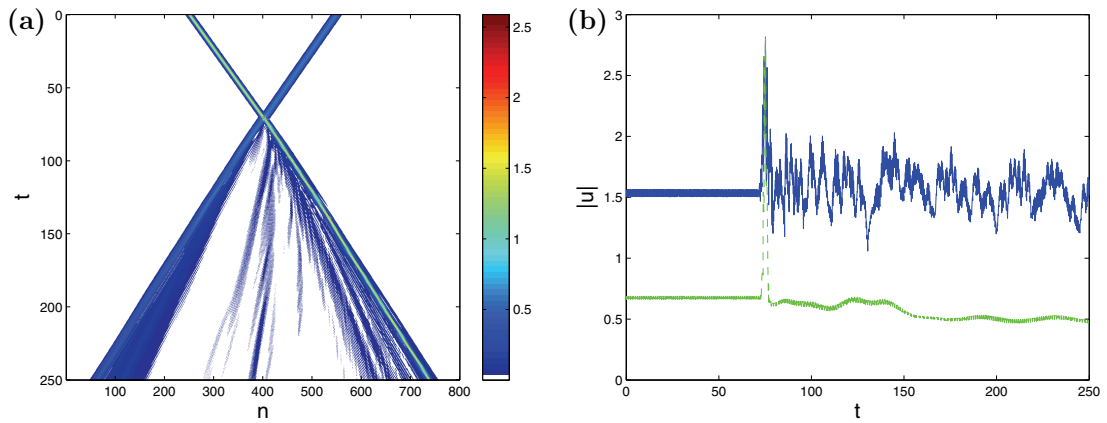

Figure 13. (a) *Collision between a single-humped and a reflected multihumped solution from branch* III *for* $\alpha = 0.65$ *and* $\kappa = 0.5$ *across a lattice for* 250 *time steps.* (b) *Amplitude of each traveling wave as a function of time. The single-humped solution is shown by the solid blue line, while the multihumped solution is shown by the dashed green line.*

Stokes constant were found to converge to the point $(\alpha, \beta) = (1, \frac{\pi}{2})$, which corresponds to the integrable AL lattice. Branches of traveling wave solutions were found along continuous curves in the (α, β)-plane. All solution families with nonzero values of κ were found not to intersect with the family of traveling wave solutions of the AL lattice. This result agrees with the Melnikov integral analysis [18], which states that the family of AL solutions at $\beta = \frac{\pi}{2}$ does not persist away from the limit $\alpha = 1$ for any finite value of κ.

We have also shown that existence curves for solutions of the differential advance-delay equation approach curves for zeros of the Stokes constant as κ gets smaller. To our knowledge, this is the first time that the relationship between the computation of Stokes constants and the numerical solutions using a pseudospectral method has been illustrated; in particular, this gives us valuable insight into the topology of the solution space. Branches of multihumped

solutions are also found for $\kappa \neq 0$ which are not predicted through analysis of the Stokes constants alone. The family of multihumped solitons joins the branch of single-humped solutions at a fold point that approaches the value $\beta = \frac{\pi}{2}$ as $\kappa \to 0$. The topology of the traveling waves in κ, β, α is interesting; there exists a number of solution "sheets" nested one behind another that contain both single- and multihumped solutions joined by a fold for some value of $\beta \leq \frac{\pi}{2}$. The single-humped solutions exist only for $\alpha > 0.5$, at least for finite κ, and are therefore separated from the cubic DNLS limit $\alpha = 0$. The multihumped solutions extend to the cubic DNLS limit. This result agrees with the center manifold analysis of the cubic DNLS [19].

Although we have shown the existence of traveling solutions in the Salerno model, there still remains the question of a full analysis of the stability and interactions of solutions. Our preliminary numerical computations show the stability of single-humped traveling waves which have near-elastic collisions and the instability of multihumped waves. The question of whether there is an infinite or finite number of solution sheets is also of interest. So far we have found four branches of solutions, but it is highly likely that, in common with the DNLS with saturable nonlinearity [14], branches of solutions would become closer together and be numerically indistinct from each other in the (α, β)-plane.

Acknowledgment. The authors would like to thank Robert McKay (Warwick) for useful conversations.

REFERENCES

[1] M. J. Ablowitz and J. F. Ladik, *Nonlinear differential-difference equations and Fourier analysis*, J. Math. Phys., 17 (1976), pp. 1011–1018.

[2] A. A. Aigner, A. R. Champneys, and V. M. Rothos, *A new barrier to the existence of moving kinks in Frenkel-Kontorova lattices*, Phys. D, 186 (2003), pp. 148–170.

[3] D. N. Christodoulides, F. Lederer, and Y. Silberberg, *Discretizing light behaviour in linear and nonlinear waveguide lattices*, Nature, 424 (2003), pp. 817–823.

[4] S. V. Dmitriev, P. G. Kevrekidis, B. A. Malomed, and D. J. Frantzeskakis, *Two-soliton collisions in a near-integrable lattice system*, Phys. Rev. E (3), 68 (2003), 056603.

[5] E. J. Doedel, A. R. Champneys, T. F. Fairgrieve, Y. A. Kuznetsov, B. Sandstede, and X. Wang, *AUTO97: Continuation and Bifurcation Software for Ordinary Differential Equations*, ftp://ftp.es.concordia.ca/directory/doedel/auto, 1997.

[6] D. B. Duncan, J. C. Eilbeck, H. Feddersen, and J. A. D. Wattis, *Solitons on lattices*, Phys. D, 68 (1993), pp. 1–11.

[7] J. C. Eilbeck and R. Flesch, *Calculation of families of solitary waves on discrete lattices*, Phys. Lett. A, 149 (1990), pp. 200–202.

[8] S. Flach and K. Kladko, *Moving discrete breathers?*, Phys. D, 127 (1999), pp. 61–72.

[9] J. W. Fleischer, T. Carmon, M. Segev, N. K. Efremidis, and D. N. Christodoulides, *Observation of discrete solitons in optically induced real time waveguide arrays*, Phys. Rev. Lett., 90 (2003), 023902.

[10] J. Gómez-Gardeñes, L. M. Floria, M. Peyrard, and A. R. Bishop, *Nonintegrable Schrödinger discrete breathers*, Chaos, 14 (2004), pp. 1130–1147.

[11] J. Gómez-Gardeñes, B. A. Malomed, L. M. Floria, and A. R. Bishop, *Discrete solitons and vortices in the two-dimensional Salerno model with coupling nonlinearities*, Phys. Rev. E (3), 74 (2006), 036607.

[12] P. G. Kevrekidis, K. O. Rasmussen, and A. R. Bishop, *The discrete nonlinear Schrödinger equation: A survey of recent results*, Internat. J. Modern Phys. B, 15 (2001), pp. 2833–2900.

[13] T. R. O. Melvin, A. R. Champneys, P. G. Kevrekidis, and J. Cuevas, *Radiationless travelling waves in saturable nonlinear Schrödinger lattices*, Phys. Rev. Lett., 97 (2006), 124101.

[14] T. R. O. Melvin, A. R. Champneys, P. G. Kevrekidis, and J. Cuevas, *Travelling solitary waves in the discrete Schrödinger equation with saturable nonlinearity: Existence, stability and dynamics*, Phys. D, 237 (2008), pp. 551–567.

[15] O. F. Oxtoby and I. V. Barashenkov, *Moving solitons in the discrete nonlinear Schödinger equation*, Phys. Rev. E (3), 76 (2007), 036603.

[16] I. E. Papacharalampous, P. G. Kevrekidis, B. A. Malomed, and D. J. Frantzeskakis, *Soliton collisions in the discrete nonlinear Schrödinger equation*, Phys. Rev. E (3), 68 (2003), 046604.

[17] D. Pelinovsky, *Translationally invariant nonlinear Schrodinger lattices*, Nonlinearity, 19 (2006), pp. 2695–2716.

[18] D. E. Pelinovsky, T. R. O. Melvin, and A. R. Champneys, *One-parameter localized traveling waves in nonlinear Schrödinger lattices*, Phys. D, 236 (2007), pp. 22–43.

[19] D. E. Pelinovsky and V. M. Rothos, *Bifurcations of travelling breathers in the discrete NLS equations*, Phys. D, 202 (2005), pp. 16–36.

[20] M. J. D. Powell, *A hybrid method for nonlinear algebraic equations*, in Numerical Methods for Nonlinear Algebraic Equations, Gordon and Breach, London, 1970, pp. 87–114.

[21] M. Salerno, *Quantum deformations of the discrete nonlinear Schrödinger equation*, Phys. Rev. A, 46 (1992), pp. 6856–6859.

[22] A. Tovbis, M. Tsuchiya, and C. Jaffé, *Exponential asymptotic expansions and approximations of the unstable and stable manifolds of singularly perturbed systems with the Hénon map as an example*, Chaos, 8 (1998), pp. 665–681.